

Casaburi, A., Heath, R. M., Ejrnaes, M., Nappi, C., Cristiano, R., and Hadfield, R. H. (2015) Experimental evidence of photoinduced vortex crossing in current carrying superconducting strips. *Physical Review B*, 92(21), 214512

There may be differences between this version and the published version. You are advised to consult the publisher's version if you wish to cite from it.

<http://eprints.gla.ac.uk/114665/>

Deposited on: 22 January 2016

Experimental evidence of photo-induced vortex crossing in current carrying superconducting strips

A Casaburi^{1,*}, R M Heath¹, M Ejrnaes², C Nappi², R Cristiano² and R H Hadfield¹

¹ *University of Glasgow - School of Engineering, Glasgow G12 8LT (UK)*

² *CNR – SPIN Institute of Superconductors, Oxides, and Other Innovative Materials and Devices, 80078 Pozzuoli, Napoli, Italy*

We report an experimental investigation that shows how magnetic vortices are generated and cross a current-carrying superconducting strip when illuminated by a bright (\sim MeV) and fast (<500 ps duration) infrared light pulse. The work has been carried out using a *strike-and-probe* electro-optic technique on a device consisting of a parallel superconducting strip configuration, with wide spacing between the strips to allow the interaction of the photons with single strip. We find that photons hitting one strip induce a collective current redistribution in the parallel strips, which we can quantitatively account for in the framework of the London model by including the effect of generated and trapped magnetic vortices in the superconducting loops formed by the two adjacent slots. The amount of trapped vorticity and its dependence on increasing current density flowing in the illuminated strip is in good agreement with the photon-assisted unbinding of vortex-antivortex pairs. This work allows us to gain a deeper understanding of the interaction between photons and current-carrying superconducting strips.

PACS numbers: 74.78.-w; 85.25.Pb; 74.90.+n

I. INTRODUCTION

The potential of superconducting strips as a basis for detection of energetic particles dates back to the 1940s, when a superconducting wire was first used in alpha particle detection [1]. The idea of photon-assisted vortex de-pairing in superconductors strips was introduced several decades ago as a possible consequence of the interaction between light and current-carrying superconductors [2]. The topic is of renewed research interest for a variety of advanced detection applications, including superconducting nanowires (SSPDs or SNSPDs) [3] for infrared single photon detection and microscopic superconducting strips for high energy (~ 20 KeV) particle or single molecule detection [4]. Such superconducting strips based devices can be fabricated with high yield over large areas with modern micro- and nanofabrication techniques. Furthermore, owing to recent advances in cryogenic engineering, these next generation superconducting detectors are increasingly being adopted for real world applications.

In the context of SNSPDs, the question of the interaction of photons with superconducting materials is critical. This holds the key for optimising the mechanism for efficient detection at near- and mid infrared photon energies [5,6] in superconducting single photon detectors (SSPDs or SNSPDs) based on nanoscale superconducting strips [3,7,8]. Theoretical investigations [9-13] have improved understanding of the different magnetic vortices that are generated and cross the superconducting element during single photon absorption. Experimentally, the main signatures of a photon assisted vortex-based detection process so far observed include the characteristic decrease in quantum efficiency with photon wavelength [14,15] and the temperature dependence of the current scale that characterizes the detection [16]. Very recent experiments have also reported evidence for a vortex-based detection process through measurements of the magnetic field dependence of the quantum efficiency [17-20] as well as its position dependence within the superconducting element [21]. A review on the detection mechanisms of SSPDs has been recently published [22].

Superconducting strips have been also used in the detection of biological macromolecules for application in time-of-flight mass spectrometry [23-25]. Here, the evidence is for a detection mechanism where the output pulses are generated through the “hot-spot” formed by high-energy phonons produced when the molecules impact the strip [26,27]. The major difference between superconducting strips and SNSPDs is related to the size of the superconducting strips (strips are five times thicker and an order of magnitude wider) and in the energy of the molecules, which is generally about a tenth of keV. In this work, the width and thickness of the strips are

very similar to those used in experiments of single-keV molecule detection, allowing for high-flowing current in the strip (\sim mA) and then large pulse amplitudes for easy detection and high signal-to-noise ratio. Nevertheless, our results could shed light on vortex dynamics induced in SNSPD by the absorption of single infrared photons as predicted from the phenomenological model developed in [2] that is still valid for disordered 3D superconducting strip. Moreover, we use a substrate having optical absorptance of 0 % at the wavelength 1550 nm, meaning that although the power of laser pulse used is very high (\sim MeV) the main interaction of photon is in the superconducting strips and no absorption occurs in the substrate.

In this experiment we use an innovative approach to experimentally investigate whether magnetic vortices have been formed in a current-carrying superconducting strip after photon impact. Our method is to illuminate thick, wide single superconducting strips using a parallel configuration with wide spacing between them where the vortex-antivortex pairs (VAPs) that are nucleated and cross the hit strip can be trapped. We can then calculate the magnitude of trapped vorticity from the measurement of the current distribution in the parallel strips. We effectively find that VAPs are nucleated after photons hit the strip being trapped then in the adjacent spacing and more VAPs are trapped when the current of the illuminated strip increases, in agreement with photon-induced VAP creation model [2].

II. FABRICATION AND EXPERIMENTAL SET UP

The specially-designed parallel strip device used in this study is shown schematically in Fig. 1. The device is based on NbN thin film deposited by DC reactive magnetron sputtering on an MgO substrate. The device structure is defined by electron beam lithography and reactive ion etching. It is made of six parallel strips having thickness $d = 40$ nm, width $w = 1$ μ m, length $l = 200$ μ m and spaced by $\Delta x = 5$ μ m for a pitch $p = 6$ μ m ($p = \Delta x + w$) (see Fig. 1 (a)). The spacing is chosen to guarantee that only one strip is struck when the focused laser beam is aligned with the center of the selected strip. The device has a critical current $I_c = 29.6$ mA and critical temperature $T_c = 15.6$ K.

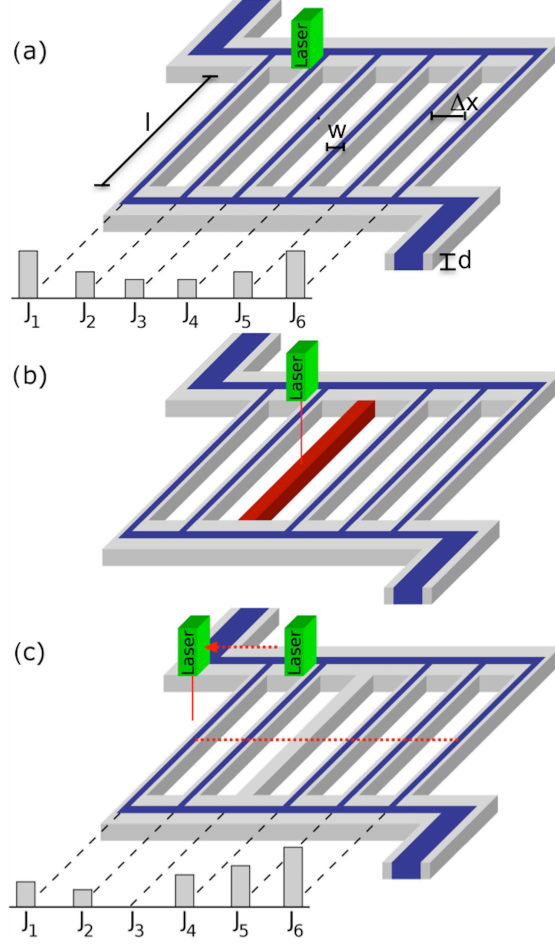


Fig 1 - Schematic of the *strike-and-probe* technique with the main sequence of steps. The blue lines indicate the currents. (a) The device is biased and the histogram shows the initial current distribution before laser illumination [28]. The laser is off and positioned on a selected strip j (in this case $j = 3$). (b) A laser pulse strikes the selected strip j ($= 3$) and an output signal is recorded. (c) The laser is then moved to the probe strip i (in this case $i = 1$) and a second laser pulse is delivered. The current that flows in this probe-strip is obtained by registering the generated voltage pulse. The probing is repeated 1,000 times to obtain a statistically-accurate value. The histogram is obtained by repeating the procedure of strip $i = 1$ for the strips $i = 2, 4, 5, 6$. The current is reset to zero after each iteration and the selected strip (the struck-strip $j = 3$ in our case) is first illuminated to re-establish the initial condition.

The electro-optic measurements were carried out by using the *strike-and-probe* technique that relies on two main components: a specially designed *parallel-superconducting-strip* geometry and the use of a nano-optical technique for precision movement and positioning of the focused laser beam on the single strips [28]. The nano-optical technique employed in this study used a fiber-based miniature confocal microscope integrated in a closed-cycle Pulse Tube (PT) refrigerator operating at $T = 3.2$ K. The miniature confocal microscope is mounted on a double piezoelectric XY scanner that provides precision movement across the whole device area. A 50 mW CW laser diode controlled by a fast electric pulse generator were used to generate the laser pulses with temporal width less than 400 ps and an energy per pulse of about 10 MeV to excite the strips; the diameter of the focused laser spot is $1.30 \pm 0.36 \mu\text{m}$ (FWHM) with the PT cold head switched on [29]. In setting up the experiment we use the confocal microscope to obtain a reflection map of the device to precisely locate the coordinates of the center position for the six strips. For more detail on the experimental set up see ref. 29 and references therein.

A key aspect of the *strike-and-probe* measurement is that when current above a certain threshold flows through a strip, i , an impinging laser pulse hitting the strip generates a voltage pulse with an amplitude, A_i , that is proportional to the current density in the strip, J_i . We use this to measure the initial current distribution as in ref. [28]. We then proceed to measure the current distribution in the strips after that the first switching event has occurred in a specific strip, j , using two laser pulses to perform the *strike and probe* measurement. The first laser

pulse is used to strike strip j and redistribute its current in the other strips whereas the second is used to probe the current in the other strip i after the redistribution has taken place. We do this in the following steps. 1) First we bias the device from zero to the operation point (Fig. 1 (a)) and the current distributes according with the shown histogram. 2) Then, the laser is positioned on the strip j , we strike it with a first laser pulse and register the voltage pulse (the *strike* of $j = 3$ – Fig. 1 (b)). 3) The laser is moved from the strip j to the strip i , which is then struck with a second laser pulse and the resulting voltage pulse height, A_i (the *probe* – Fig. 1 (c)) is measured. 4) At this point we bias the device at zero current to reset the current and return to the initial condition and 5) we can now repeat the steps 1 - 4 1,000 times to obtain a more accurate statistics and improve the precision of the A_i measurement by averaging. 6) We repeat steps 1 - 5 for all the strips $i \neq j$. At this point we have measured all the pulse heights from the strips $i \neq j$ for the case of when strip j has generated the first detection event.

III. MEASUREMENTS

The first measurement we perform is that of the initial current distribution in the six parallel strips (see the black triangles in Fig. 2) from which we calculate an effective London penetration depth of $12.3\mu\text{m}$ in agreement with previous measurements [28]. This current distribution can be obtained only with no trapped vortices (vorticity) present in the slots adjacent the strips. Therefore we can say that no residual vorticity is introduced in the device during the cool down also if no magnetic shielding is used.

We observe that the measured pulse amplitudes increase linearly with an increase of the current flowing in the strip, i.e. $A_i \propto I_i$ [28]. Furthermore, in the *strike-and-probe* measurements we have observed that the struck strip does not generate signal pulses if it is repeatedly struck again, unless another strip is struck. This means that there is a significant reduction in the current flowing through a struck strip. We therefore assume that it is zero. From the above considerations, the equivalence between normalized signal amplitudes and normalized current densities can be established:

$$\frac{A_i}{\sum A_i} = \frac{J_i}{\sum J_i}.$$

This allows us to infer the normalized current density in each strip by measuring the pulse amplitude generated when a laser pulse strikes it.

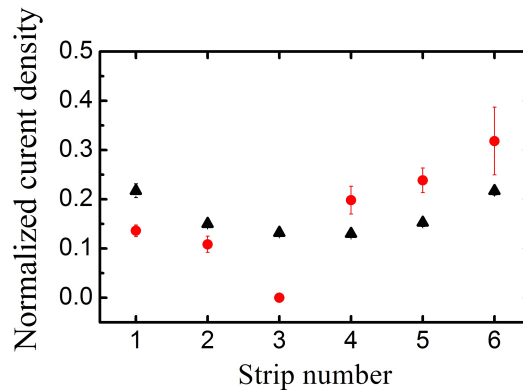


FIG 2. (a) Measured initial current distribution in the six strips (black triangle) and measured current redistribution after the $j = 3$ was struck (red dots).

We then measure the current redistribution in the device after a light pulse has struck a generic strip. In Fig. 2 for instance, we show the current redistribution after the strip $j = 3$ has been hit (red dots). The black triangles show the initial current distribution. From the measurements, we see that the current distribution has changed from the initial one and that it involves *all* the parallel strips in different ways. Hence, a detection event in strip 3 actually *lowers* the current in strips 1 and 2, whereas the current *increases* in strips 4, 5 and 6. This shows that during this process, the current that was present in strip 3 does not simply flow into the other strips after the detection event but rather a *collective* current redistribution occurs within the six parallel strips.

To further investigate this phenomenon we have measured the current redistribution when each of the strips 1, 2, 3 and 4 was initially struck and the results are shown in Fig. 3 (a) – (d) respectively. We note that by symmetry of the device the results of striking initially strip 4 should be the mirror image of what we observe when striking first strip 3 and this is indeed the case. Also, when strip 2 was initially struck we observe the current in strip 1 becomes lower than it was initially, indicating that the current is redistributed collectively. In the next section, we show that a key feature for the interpretation of these measurements in the framework of the London model is to introduce the presence of vorticity in the basic equation of the generalized London theory [30].

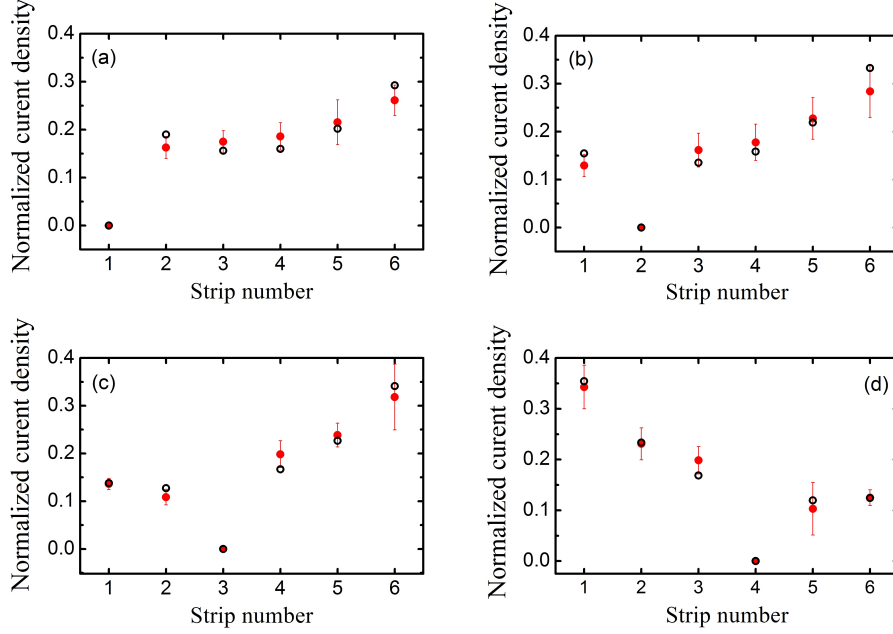


FIG 3. (color online) Normalized measured (red dots) and calculated (black circle) current density as a function of the strip number. The four panels refer to different struck-strips j : (a) $j = 1$, (b) $j = 2$, (c) $j = 3$ and (d) $j = 4$ respectively. The calculated current density values are obtained from the modified London theory using $a = 0.239$, fixing the current density in the struck-strip equal to zero and fitting the experimental data with the normalized vorticity v_i as the only free parameter.

IV. THEORETICAL MODEL AND DISCUSSION

The generalized form of London theory is represented by the equation [30]:

$$\nabla \times (\mu_0 \lambda^2 \mathbf{J}) + \mathbf{B} = \mathbf{V}(\mathbf{r} - \mathbf{r}_i). \quad (1)$$

The vorticity term $\mathbf{V}(\mathbf{r} - \mathbf{r}_i)$ accounts for the presence of magnetic field sources located at the generic positions \mathbf{r}_i . Here λ is the London penetration depth. In what follows we show that vortices and the associated vorticity play a fundamental role in understanding the observed phenomenology. The emerging picture is that when the laser pulse strikes the strip, magnetic vortices nucleate and remain trapped in the superconducting loops formed by the two slots next to the struck strip. The presence of trapped vortices influences the current distribution, and can be quantified by using its vorticity to fit the measured data. We use the hypothesis that $\mathbf{J} = J(x)\mathbf{e}_y$ and therefore

$$\nabla \times \mathbf{J} = \frac{\partial J(x)}{\partial x} \mathbf{e}_z.$$

Since $\mathbf{B} = B(x)\mathbf{e}_z$ so that $\mathbf{V}(\mathbf{r}) = V(x)\mathbf{e}_z$, in our case the Eq. (1) can be written as

$$\mu_0 \lambda^2 \frac{\partial J(x)}{\partial x} + B(x) = V(x). \quad (2)$$

It is convenient to eliminate $J(x)$ from Eq.(2) and write an equation in terms of $B(x)$. In this way we avoid derivatives of $V(x)$. Using Ampère's law, and remembering that $\mu_0 \mathbf{H} = \mathbf{B} = B(x)\mathbf{e}_z$, Eq. (2) can be written as

$$B(x) - \lambda^2 \frac{\partial^2 B(x)}{\partial x^2} = V(x) \quad (3)$$

or, taking finite differences, as

$$(2 + a)B_i - B_{i+1} - B_{i-1} = aV_i \quad i = 1, 2 \dots 5 \quad (4)$$

where B_i is the magnetic induction and V_i is the vorticity in the spacing between the strips i and $i+1$. To close the system of equations, we use the integral form of the Ampère's law, i.e.

$$-\mu_0 \Delta x \frac{I_{bias}}{wd} = B_6 - B_0 \quad (5)$$

where B_0 and B_6 are the values of the magnetic induction at the two lateral external sides of the device. We also assume that

$$\sum_{i=1}^5 B_i = B_{tot}. \quad (6)$$

Eq. (5) and (6) plus the five relations of Eq.(4) permits the calculation of the seven B_i values. Our aim, however, is the calculation of J_i , the current densities in the six strip-lines that can be obtained from

$$-\mu_0 \Delta x J_i = B_i - B_{i-1} \quad i = 1, 2 \dots 6. \quad (7)$$

The J_i values are obtained in terms of the four parameters I_{bias} , B_{tot} , a and V_i . I_{bias} is fixed in the experiment and the value $a = 0.239$ is obtained from the measured initial current distribution [28].

The model [Eqs. (4) – (6)] is very general and we restrict it to describe the experiment by assuming that after striking the strip j , two things occur: 1) the current flowing in the strip becomes zero, $J_j = 0$, and 2) the device traps only two vortices with opposite vorticity in the adjacent holes, $V_j = -V_{j-1}$. The first assumption is suggested by the observation that *only* the first laser shot in a sequence generates a signal pulse from the struck strip and this permits solution of the equation $J_j(V_j, I_{bias}, a, B_{tot}) = 0$ for B_{tot} . The second assumption, i.e. the formation of a pair of opposing vorticity, is used to set to zero all V_i with $i \neq j, j-1$. Thus, the only free parameter in the model is the value of the vorticity V_j at the site j . Since we measure signal pulse amplitudes and compare them with calculated current densities, it is appropriate to use normalized quantities. The fitting parameter V_j is also normalized to be cast as a dimensionless quantity, i.e.

$$v_j = a \frac{V_j}{\mu_0 \Delta x \frac{I_{bias}}{wd}}.$$

We can thus obtain the best-fit value, using a least-squares procedure with a single parameter (the normalized vorticity, v_j) that describes the current distribution when strip-line j has been struck. In Fig. 3 we show the current distributions calculated for the best-fit values: $v_1 = 0.27 \pm 0.03$, $v_2 = 0.14 \pm 0.02$, $v_3 = 0.15 \pm 0.03$ and $v_4 = 0.14 \pm 0.02$. The calculated distribution for the case of striking strip 1 is distinct because there is no hole on the left side of the strip and it was obtained by considering trapped vorticity only in the hole next to

the strip. As can be seen, the theoretical distributions fit very well the experimental points and reproduce many phenomenological characteristics of the physical system. As expected, the predicted current distributions are twofold degenerate: distributions for striking strip 1, 2 or 3 are mirror images of the ones where strip 6, 5 or 4 was struck respectively [see Fig. 3(c) and 3(d)]. We note that the inclusion of the effect of vortices is crucial in our analysis in order to replicate the experimental data in a satisfactory way. Any attempt to reproduce the data within the London model, which does not rely on finite vorticity, failed.

The obtained values for v_i for the cases $i = 2, 3$ and 4 are quite similar to each other whereas v_1 is almost double the rest. To investigate further this point, we now do the hypothesis that vortices nucleate and cross the hit strip as figured out by the model of SNSPD detection mechanism [23]. The current density flowing in the struck strip lowers the unbinding energy, $U(J)$, for a vortex-antivortex pair at a level comparable to that of a single photon at wavelength of 1550 nm: $E_{\text{photon}} \sim 0.8 \text{ eV} > U(J)$. This energy can be roughly calculated as $U(J) \sim 2\pi K_0 \ln(J_c/J)$ [2]. Here $2\pi K_0 \sim \Phi_0 d \xi J_c$ where ξ is the Ginzburg-Landau coherence length ($\sim 5 \text{ nm}$ for the NbN) and Φ_0 is the magnetic flux quantum. We calculate the following values for the VAP unbinding energy for the different strips: $U(J_{1,6}) = 0.181 \text{ eV}$, $U(J_{2,5}) = 0.328 \text{ eV}$ and $U(J_{3,4}) = 0.416 \text{ eV}$ respectively. At the operating temperature $T = 3.5 \text{ K}$ (that corresponds to a ratio $T/T_c = 0.23$) the thermal energy fluctuations are small compared to $U(J)$, $k_B T \sim 300 \text{ } \mu\text{eV}$, and therefore the probability of VAP generation via thermal processes is vanishingly small. At this point each photon could produce several pairs of free vortices in proportion to $U(J_i)$, which can then be swept to the sides of the strip by the transport current. For the hypothesis that each photon has a certain probability of generating an average number of vortices we can assume that $v_i \propto E_{\text{pulse}}/U(J_i)$, where E_{pulse} is the energy of the laser pulse which is kept constant in the experiment. This allows us to compare the calculated ratio $U(J_2)/U(J_1) = 1.81$ to the ratio of the measured vorticity $v_1/v_2 = 1.85 \pm 0.05$ and we find a good agreement showing that it is likely that trapped vortices originate as photo-induced unbound vortices in the strip-lines. We cannot analyze the ratio $U(J_2)/U(J_3)$ in the same way because the relative difference in the calculated values induces a variation in the trapped vorticity comparable to the experimental error. For example, $[U(J_3) - U(J_2)] / U(J_3) = 0.211 = (v_2 - v_3) / v_2$ which in turn should induce a variation in the normalized vorticity of $v_2 - v_3 = 0.03$ which is about the experimental error in the vorticity values. The trapped VAPs govern the current distribution occurring among parallel strips after a detection event and the number of VAPs nucleated from the strip is directly related to the current density flowing in the strip when the light pulse struck it.

We have also calculated the energy of the system for the different current distributions and investigated how this changes with the variation of v_i when the strip i has been struck. In order to do this we use the formula

$$E = \frac{1}{2\mu_0} \int_V [B^2 + \mu_0^2 \lambda^2 J^2] dV$$

that gives the energy within the volume of the device. The two terms are the magnetic energy due to the induced magnetic flux B and kinetic energy due to the flowing current density J . This equation can be rewritten for our system as [31]:

$$E = \frac{1}{2\mu_0} \left[l d \Delta x \sum_{j=1}^5 B_j^2 + \mu_0^2 w l d \lambda^2 \sum_{j=1}^6 J_j^2 \right] \quad (9)$$

In Fig. 4 we plot the calculated energies with variation of the v_j values for the current distributions shown in the Fig. 3 corresponding to the struck-strips $j = 1, 2$ and 3. Due to the twofold degeneracy of the current distribution for $j = 3$ and $j = 4$, the corresponding v_4 curve of the energy is identical and has not been shown. It can be seen from Fig. 4 that the generation of vorticity is energetically favorable in all cases because the minimum energy when the current is redistributed is reached for vorticity values approximately equal to those obtained from our fitting procedure.

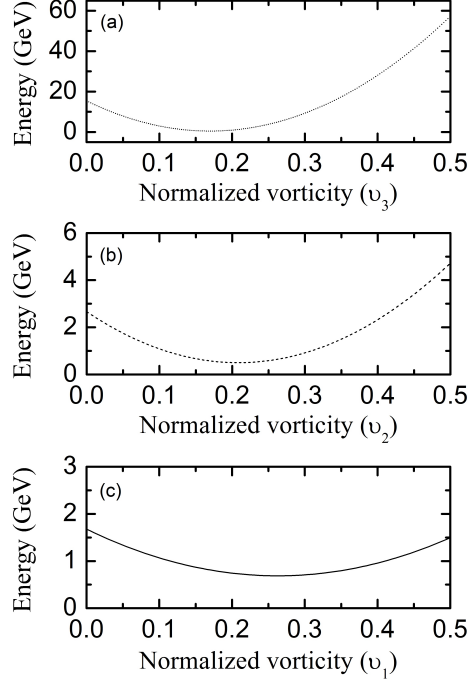


FIG 4. Energy stored in the system as function of vorticity. The different curves refer to the cases where the struck strip was $j = 3$ (a), $j = 2$ (b) and $j = 3$ (c). The minima in the curves are located at vorticity values in qualitative agreement with the values obtained by the best fit procedure.

V. CONCLUSIONS

We have performed *strike-and-probe* measurements on a specially designed device having parallel strips and large slots between them to investigate the effect generated by the absorption of infrared photons in superconducting current-carrying strips. The thick and wide strips allow us to firstly detect and measure the amplitude of the pulses induced by laser pulses and secondly, to determine the resulting current distribution in the parallel strips. By measuring the current redistribution occurring after photon impact on the strips we clearly see that current does not simply flow into the other parallel strips but rather a *collective* current redistribution takes place. Only when we include effect of trapped magnetic vortices in the adjacent slots we can account for the measured current distributions using the generalized London model. This comparison between our experimental results and the model strongly indicates that vortices are generated and cross an illuminated current carrying superconducting strip. The adjacent slots act as superconducting loops, trapping the photo-induced vortices allowing us to measure and quantify their presence from measuring the current distribution. The experimental results are in agreement with the hypothesis of creation- and crossing of VAPs in the illuminated superconducting strip as described in the model of ref. 2 developed more generically for disordered 2D/3D current-carrying superconducting strips. We find also that the amount of trapped vorticity increases with the current density of the illuminated strip in agreement with that model [2].

It is interesting to consider the relevance of this study to the current debate on the mechanism of infrared single photon detection in SNSPDs. In our study reported here, the superconducting strips studied have width of about 10 times- and thickness of about 8 times greater than those used for the SNSPDs. Our device is a 3D disordered superconducting structure; a typical SNSPD is a 2D disorder superconducting structure. Our device configuration allows current flow in each strip (\sim mA) and produces large pulse amplitudes for easy detection and high signal-to-noise ratio. Nevertheless, our results could shed light on vortex dynamics induced in SNSPD by the absorption of single infrared photons since the general validity of the model developed in the ref. 2 of manuscript that is valid for *both* 2D and 3D disordered superconducting strips. Moreover no significant heating effect occurs neither in the substrate (0 % of photons at 1550 nm wavelength are absorbed in the substrate) nor in the strip. The high power pulse (MeV) can be regarded as a large number of photons ($\sim 10^6$) impinging on the strips. Due to the small bias current ($I_B/I_C = 0.63$), a much smaller fraction of this photons ($\sim 10^3$) impinging on

an area of about $2 \mu\text{m}^2$ generates VAPs with a certain probability just like in SNSPDs. The high number of photons (VAPs) allow sufficient vorticity to be generated, leading in turn to a current redistribution that can be easily measured. Therefore, this study indicates that the most probable mechanism when optical radiation strikes a superconducting strip/nanowire is generation and crossing of VAPs. This study therefore supports the hypothesis that for SNSPDs magnetic vortices play a dominant role in the detection mechanism as recently reported in literature [23].

As a final conclusion, it is also worth noting the wider potential of the experimental technique employed in our study. Our low temperature nano-optical setup up allows us to address a microscopic area of the device, and controllably investigate the device response through a strike-and-probe procedure. The ability to stably trap photo-induced vorticity makes this device configuration very promising as an ideal test-bed for gaining a deeper understanding of future experimental investigations concerning the interaction of current carrying superconductors with photons or energetic particles. We hope to apply this technique to new superconducting materials and device configurations in the future.

ACKNOWLEDGEMENTS

AC acknowledges a Marie Curie Intra European Fellowship. RHH acknowledges a Royal Society University Research Fellowship and support through UK Engineering and Physical Society grants EP/J007544/1 and EP/L024020/1.

References

- [1] D. H. Andrews, R. D. Fowler, and M. C. Williams, *Phys. Rev.* **76**, 154 (1949)
- [2] A.M. Kadin, M. Leung and A.D. Smith, *Phys. Rev. Lett.* **65**, 3193 (1990)
- [3] C.M. Natarajan, M.G. Tanner and R.H. Hadfield, *Supercond. Sci. Technol.* **25**, 063001 (2012)
- [4] K. Suzuki, S. Miki, S. Shiki, Z. Wang and M. Ohkubo *Applied Physics Express* **1**, 031702 (2008)
- [5] F. Marsili, V.B. Verma, J.A. Stern, S. Harrington, A.E. Lita, T. Gerrits, I. Vayshenker, B. Baek, M.D. Shaw, R.P. Mirin and S.W. Nam, *Nat. Photon.* **7**, 210 (2013)
- [6] W.H.P. Pernice, C. Schuck, O. Minaeva, M. Li, G. N. Goltsman, A.V. Sergienko and H.X. Tang, *Nat. Commun.* **3**, 1325 (2012)
- [7] R.H. Hadfield, *Nat. Photon.* **3**, 696 (2009)
- [8] M.D. Eisaman, J. Fan, A. Migdall and S.V. Polyakov, *Rev. Sci. Instrum.* **82**, 071101 (2011) L.N. Bulaevskii, M.J. Graf, C.D. Batista and V.G. Kogan, *Phys. Rev. B* **83**, 144526 (2011)
- [9] L.N. Bulaevskii, M.J. Graf and V.G. Kogan, *Phys. Rev. B* **85**, 014505 (2012)
- [10] A. Gurevich and V.M. Vinokur, *Phys. Rev. B* **86**, 026501 (2012)
- [11] A.N. Zotova and D.Y. Vodolazov, *Phys. Rev. B* **85**, 024509 (2012)
- [12] D.Y. Vodolazov, *Phys. Rev. B* **90**, 054515 (2014)
- [13] A. Engel, J. Lonsky, X. Zhang and A. Schilling, *IEEE Trans. Appl. Supercond.* **25**, 2200407 (2015)
- [14] A.D. Semenov, P. Haas, H.-W. Hübers, K. Ilin, M. Siegel, A. Kirste, T. Schurig and A. Engel, *Physica C* **468**, p. 627 (2008)
- [15] M. Hofherr, D. Rall, K. Ilin, M. Siegel, A. Semenov, H.-W. Hübers and N.A. Gippius, *J. Appl. Phys.* **108**, 014507 (2010)
- [16] J.J. Renema, R. Gaudio, Q. Wang, Z. Zhou, A. Gaggero, F. Mattioli, R. Leoni, D. Sahin, M.J.A. de Dood, A. Fiore and M.P. van Exter, *Phys. Rev. Lett.* **112**, 117604 (2014)

- [17] A. Engel, A. Schilling, K. Il'in and M. Siegel, Phys. Rev. B **86**, 140506(R) (2012).
- [18] R. Lusche, A. Semenov, Y. Korneeva, A. Trifonov, A. Korneev, G. Gol'tsman, and H.-W. Hubers, Phys. Rev. B **89**, 104513 (2014).
- [19] J.J. Renema, R.J. Rengelink, I. Komen, Q. Wang, R. Gaudio, K.P.M. op 't Hoog, Z. Zhou, D. Sahin, A. Fiore, P. Kes, J. Aarts, M.P. van Exter, M.J.A. de Dood and E. F. C. Driessen, Appl. Phys. Lett. **106**, 092602 (2015)
- [20] D.Yu. Vodolazov, Yu.P. Korneeva, A.V. Semenov, A.A. Korneev and G. N. Goltsman, arXiv:1505.04689v1
- [21] J.J. Renema, Q. Wang, R. Gaudio, I. Komen, K. op 't Hoog, D. Sahin, A. Schilling, M.P. van Exter, A. Fiore, A. Engel, and M.J.A. de Dood, Nanoletters **15**, 4541 (2015)
- [22] A. Engel, J. J. Renema, K. Il'in and A. Semenov, Supercond. Sci. Technol. **28**, 114003 (2015).
- [23] A.Casaburi, N. Zen, K. Suzuki, M. Ejrnaes, S. Pagano, R. Cristiano and M. Ohkubo, Appl. Phys. Lett. **94**, 212502 (2009)
- [24] N. Zen, A.Casaburi, K. Suzuki, M. Ejrnaes, S. Pagano, R. Cristiano and M. Ohkubo, Appl. Phys. Lett. **95**, 172508 (2009)
- [25] A. Casaburi, E. Esposito, M. Ejrnaes, K. Suzuki, M. Ohkubo, S. Pagano and R. Cristiano, Supercond. Sci. Technol. **25**, 115004 (2012)
- [26] K. Suzuki, S. Shiki, M. Ukibe, M. Koike, S. Miki, Z. Wang and M. Ohkubo, Appl. Phys. Expr. **4**, 083101 (2011)
- [27] A.Casaburi, N. Zen, K. Suzuki, M. Ejrnaes, S. Pagano, R. Cristiano and M. Ohkubo, Appl. Phys. Lett. **98**, 023702 (2011)
- [28] A. Casaburi, R.M. Heath, M.G. Tanner, R. Cristiano, M. Ejrnaes, C. Nappi and R.H. Hadfield, Appl. Phys. Lett. **103**, 013503 (2013)
- [29] R.M. Heath, M.G. Tanner, A. Casaburi, M.G. Webster, L. San Emeterio Alvarez, W. Jiang, Z.H. Barber, R.J. Warburton, and R.H. Hadfield, Appl. Phys. Lett. **104**, 063503 (2014)
- [30] T.P. Orlando and K.A. Delin, *Foundations of applied superconductivity*, Addison-Wesley, Reading, MA (1991), p. 268
- [31] A. Casaburi, R.M. Heath, M.G. Tanner, R. Cristiano, M. Ejrnaes, C. Nappi and R.H. Hadfield, Supercond. Sci. Technol. **27**, 044029 (2014)